Journal of Applied Electrochemistry (2019) 49:937–947
https://doi.org/10.1007/s10800-019-01336-9

RESEARCH ARTICLE

Platinum decorated polythiophene modified stainless steel for electrocatalytic oxidation of benzyl alcohol

E. K. Joice[1] · Sherin Rison[1,2] · K. B. Akshaya[2] · Anitha Varghese[2]

Received: 12 April 2019 / Accepted: 2 July 2019 / Published online: 18 July 2019

Abstract

Platinum nanoparticles were electrochemically deposited on conducting polymer polythiophene (PTh)-coated stainless steel (SS) substrate. A thin layer of PTh on the steel substrate facilitates uniform deposition of Pt nanoparticles on the substrate, thereby improving the surface area to a great extent. The electrochemical properties of the modified electrodes were analyzed by cyclic voltammetry (CV) and electrochemical impedance spectroscopy (EIS). The physicochemical properties of the modified electrodes were investigated by Scanning electron microscopy (SEM), Transmission electron microscopy (TEM), X-ray diffraction spectroscopy (XRD), Raman spectroscopy, and Fourier transform infrared spectroscopy (FTIR). The proposed method has been applied for the electrocatalytic oxidation of benzyl alcohol in the presence of a mediator, 2,2,6,6-tetramethylpiperidine 1-oxyl (TEMPO). Cyclic voltammetric studies reveal that the electrocatalytic activity of Pt–PTh/SS electrode is higher than that of PTh/SS electrode toward the conversion of benzyl alcohol to benzaldehyde.

Graphic abstract

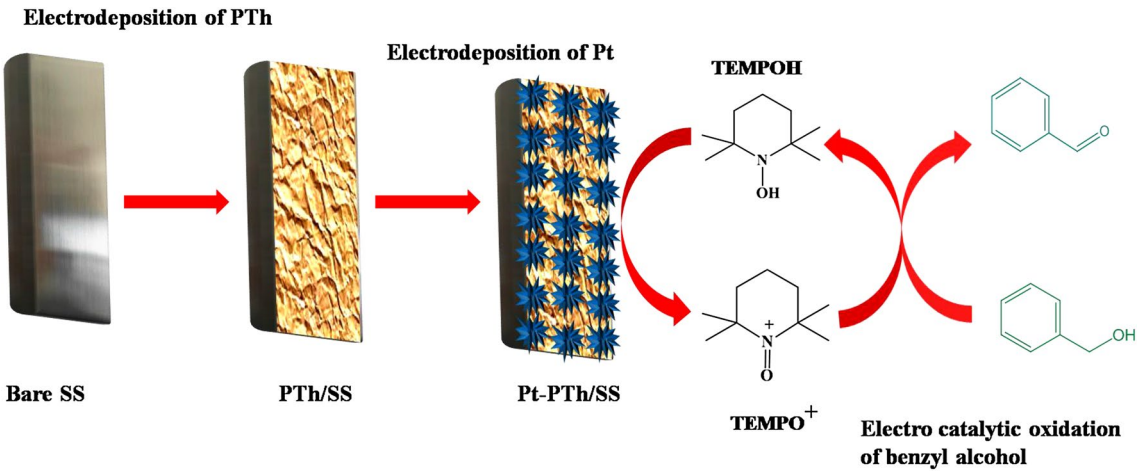

Keywords Polythiophene · TEMPO · Electrooxidation · Benzyl alcohol

1 Introduction

Conducting polymers have received immense scientific attention owing to their broad applications in the field of thin-film transistors, polymer light-emitting diodes (LEDs), corrosion resistance, electromagnetic shielding, sensor technology, molecular electronics, supercapacitors, and electrochromic devices [1]. They have been used as host matrices

✉ Anitha Varghese
anitha.varghese@christuniversity.in

[1] Christ Academy Institute for Advanced Studies, Christ Nagar, Begur–Koppa Road, Bengaluru 560083, India

[2] Department of Chemistry, CHRIST (Deemed to be University), Bengaluru 560029, India

for metal nanoparticles, complex ions, and enzyme immobilization through which the polymeric system acquires catalytic functionality [2–8]. Conducting polymers (CPs) are advantageous in terms of easier preparation by chemical and electrochemical methods and are chemically durable against aerial oxidation. It acts as a supporting material for electrocatalysis. Most of the catalytic reactions are controlled by adsorption which relies upon the nature and structure of catalytic centers. The dispersion of metal nanoparticles in CP thin films displays stronger adsorbability with the increasing surface area and catalytic efficiency due to roughening of the conducting surface [9]. The electron-transfer properties at the electrode–electrolyte interface arises from the electrons of Pt, Pd, Au, Ag, Cu, and Ni nanoparticles, which are dispersed along the chains of CP host matrix which induces porosity on the substrate electrode [10–12].

CPs such as polyaniline (PANI), polypyrrole (PPy), poly(3,4 ethylenedioxythiophene) (PEDOT), and polythiophene (PTh) have been explored as supporting host matrices for the dispersion of nanoparticles. Metal nanoparticles-dispersed CPs have earlier been reported for the oxidation of organic molecules such as folic acid, formaldehyde, and methanol [13, 14]. High stability, conductivity, and processability at ambient conditions make PTh a versatile CP for various electrocatalytic applications. PTh has been widely used in environmentally and thermally stable CP-based materials for applications such as chemical and optical sensors, light-emitting diodes and displays, photovoltaic devices, molecular devices, DNA detection, polymer electronic interconnects, solar cells, and transistors [15–17]. Its extensive electrochemical property and the control over morphology can be attributed to the electrosynthetic conditions and structural modifications. This makes PTh one of the most attractive CPs [18, 19]. The electrodeposition of a polymer with open morphology and adequate conductivity allows the incorporation of metal nanoparticles. Waltman et al. prepared highly conducting PTh films on Pt working electrode by electropolymerization and applied the same in the preparation of electroluminescent materials [20]. Dai et al. investigated the electrosynthesis of PTh film from boron trifluoride diethyl etherate (BFEE) containing thiophene monomer on the stainless steel substrate [21]. There are also reports of increased electrocatalytic efficiency for CP substrate decorated with metal nanoparticles. Kent and his coworkers immobilized Pt nanoparticle on PANI-coated glassy carbon electrode (GCE) for the oxidation and reduction of methanol [22]. Dominguez and his coworkers studied the electrodeposition of Pt nanoparticles under potentiostatic condition on several carbonaceous electrodes with PANI and poly-o-aminophenol as CPs [23]. Schrebler et al. have modified PTh on electrode substrate by electrodepositing Pt and Pt-supported lead and applied in the electrooxidation of formic acid [24]. Pt–Sn catalysts dispersed on poly(3-methyl) thiophene electrodes have also been reported for the electrocatalytic oxidation of methanol [25].

Benzaldehyde formed as a result of Benzyl alcohol oxidation is one of the industrially significant chemicals. Conventional methods that have been reported for the synthesis of benzaldehyde include liquid-phase chlorination and oxidation of toluene which results in chlorinated impurities along with the desired product [26]. The conventional synthesis of benzaldehyde from benzyl alcohol by treatment with excess of potassium permanganate resulted in production of large amount of waste [27]. Controlled oxidative conversion of benzyl alcohol to benzaldehyde is the most basic reaction involving oxygen group transfer, resulting in the formation of an aldehydic intermediate. Zhao et al. demonstrated that benzyl alcohol could be electrooxidized to benzaldehyde in a biphasic system consisting of supercritical CO_2 and ionic ligands [28]. The oxidation of benzyl alcohol which conventionally uses oxidizing agents such as Cr_2O_7, MnO_4, and SeO_2 are known to pose serious threat to the environment. These oxidizing agents can be substituted by a mediator. Oxidized TEMPO (2, 2, 6, 6-tetramethylpiperidin-1-yl)oxyl is one such mediator, which is a stable oxoammonium cation ($TEMPO^+$) in acetonitrile acting as a high-energy selective catalyst [29]. TEMPO is stable in both aqueous and non-aqueous media due to its steric hindrance around the nitrosyl moiety. TEMPO can be oxidized electrochemically, or by means of oxidants such as H_2O_2, O_2, and metal halides to generate an active oxoammonium species that reacts with alcohol resulting in the formation of an aldehyde or ketone [30]. TEMPO prevents overoxidation of Benzyl alcohol to Benzoic acid. The interconversions among TEMPO, TEMPOH (hydroxyl amine), and $TEMPO^+$, and their abilities to scavenge reactive radicals are often explored in biochemical applications [31].

In the present investigation, Pt nanoparticles were dispersed into PTh CP coated on SS substrate which has displayed remarkable electrocatalytic properties toward the oxidation of benzyl alcohol to benzaldehyde in the presence of TEMPO mediator. SS is economic, electrically conducting, and environment friendly. To the best of our knowledge, electrodepositions of Pt on PTh-coated SS are being reported for the first time for the electrocatalytic oxidation of benzyl alcohol in the presence of TEMPO mediator.

2 Experimental

2.1 Reagents

Thiophene (Th), chloroplatinic acid (H_2PtCl_6), and TEMPO were purchased from Sigma Aldrich-Merck (> 99%). Potassium ferricyanide ($K_3[Fe(CN)_6]$), potassium ferrocyanide ($K_4[Fe(CN)_6]$), and acetonitrile (ACN) were procured from

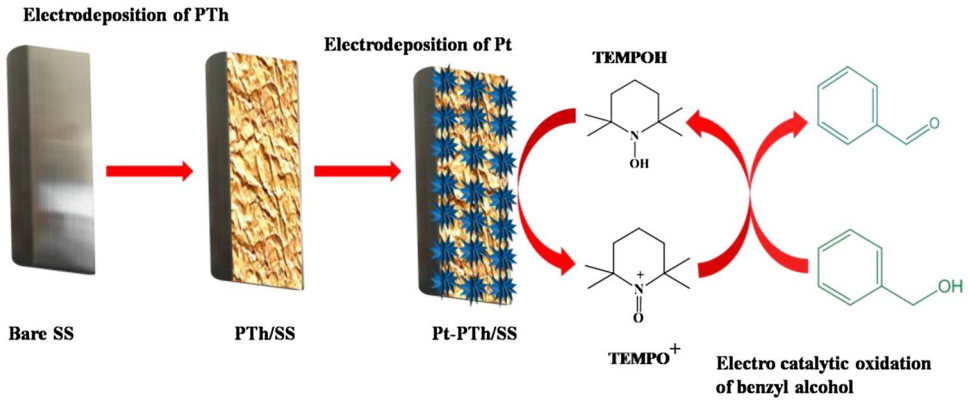

Scheme 1 Schematic representation of benzyl alcohol oxidation in the presence of TEMPO at Pt–PTh/SS electrode

SD Fine-Chemicals Pvt. Ltd. India. Extra-pure lithium perchlorate ($LiClO_4$) (99%) was bought from Loba Chemie Pvt. Ltd. India. Double-distilled water was used for preparing the aqueous solutions. A highly pure 304 grade SS foil of thickness 0.2 mm was used as the substrate for the deposition of PTh and Pt on PTh. A glass cell of 50 mL volume with suitable ground-glass joints was used to house SS or modified SS as substrate working electrode, Pt foil as counter electrode, and a saturated calomel reference electrode for the electrochemical deposition of Pt on PTh/SS and PTh, electrochemical characterization, and oxidation of benzyl alcohol. All the potential values are reported against saturated calomel electrode. Preliminary experiments were performed using polished and cleaned electrodes. Adherence onto SS sheet was improved by subjecting it to sand blasting which generated a noticeable rough surface and was washed continuously using a detergent followed by amide etching in dilute H_2SO_4. A foil of 7.0 cm in length with 1.2 cm width was sectioned out of a sand-blasted SS sheet. An area of 1.5 cm^2 at one end was exposed to the electrolyte, and the rest of its length was used as tag to make electrical contacts. The SS substrate was washed with water, rinsed with acetone, and dried in vacuum at an ambient temperature for 30 min. The electrochemical measurements were carried out at room temperature in the range 22 ± 1 °C in an air conditioned room.

2.2 Instrumentation

Cyclic voltammetric deposition of PTh on SS and Pt on PTh/SS, EIS measurements, and electrocatalytic oxidation of benzyl alcohol were performed on electrochemical analyzer CHI608E (CH Instrument Inc. USA). SEM images were recorded using FEI scanning electron microscope (model SIRION). TEM images were recorded on a JEOL/JEM2100 model TEM. Powder X-ray diffraction (XRD) patterns were obtained on a Bruker AXS D8 advanced X-ray diffractometer using Cu Kα radiation (λ = 1.5406 A°). Lab RAM HR FT Raman module was used for FT Raman spectroscopic analysis. Thermo Nicolet Avatar 370 was used to record the FTIR spectra.

2.3 Preparation of PTh/SS and Pt–PTh/SS

The electropolymerization of PTh on SS electrode was performed using a solution containing 0.1 M Th, 0.1 M $LiClO_4$ in ACN medium for 25 successive potential cycles in the range − 1.20 V to 1.80 V at a scan rate of 0.05 Vs^{-1}. After the electrodeposition, the electrode was rinsed with double-distilled water and dried. An electrolyte containing 0.005 M H_2PtCl_6 and 0.1 M H_2SO_4 was used for the electrodeposition of Pt nanoparticles on PTh/SS for 15 cycles between − 0.70 V and 1.7 V using a scan rate of 0.05 Vs^{-1}.

2.4 Electrochemical oxidation of benzyl alcohol

The behaviors of Pt-PTh/SS and other electrodes toward electrocatalytic oxidation of benzyl alcohol in the presence of TEMPO (0.01 M) in ACN medium with 0.1 M $LiClO_4$ supporting electrolyte were studied using cyclic voltammetry in the potential range − 0.62 V to 1.00 V at 0.05 Vs^{-1} scan rate. The schematic representation of benzyl alcohol oxidation at Pt–PTh/SS electrode using TEMPO has been presented in Scheme 1.

3 Results and discussion

3.1 Electrochemical preparation of Pt–PTh/SS

The electropolymerization technique can be used to control the thickness and homogeneous nature of the CP deposited on the electrode substrate. The cyclic voltammograms obtained for the electropolymerization of thiophene are shown in Fig. 1. An electrolyte containing 0.1 M thiophene, 0.1 M $LiClO_4$ as supporting electrolyte in acetonitrile was taken for the electrodeposition of PTh for 25 cycles in the potential range − 1.20 V to 1.80 V at 0.05 Vs^{-1} scan rate.

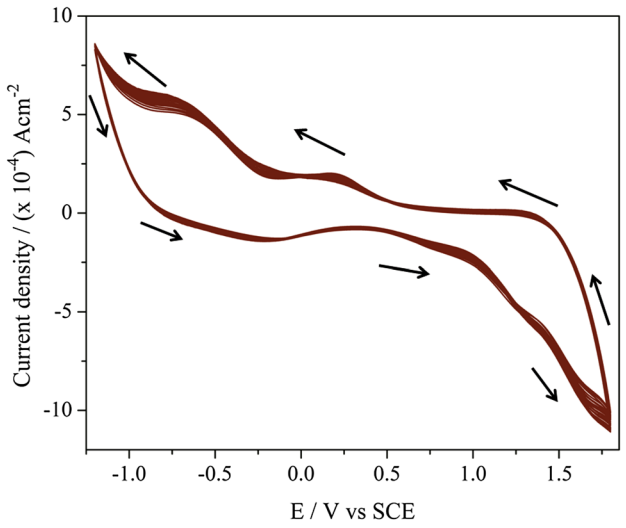

Fig. 1 Electropolymerization of thiophene on SS by 25 scanning potential cycles at a scan rate of 0.05 Vs^{-1}: (0.1 M) thiophene; (0.1 M) $LiClO_4$ in acetonitrile

As observed in the figure, the oxidation of thiophene starts at − 0.62 V generating the first layer of polythiophene. The successive cycles show progressive growth of PTh layer. The current starts to increase from 0.79 V and another oxidation peak was observed at 1.26 V. Two reduction peaks were observed at − 0.69 V and 0.22 V.

The mechanism for the electropolymerization of thiophene involves the presence of radical cations and their dimerization. In the propagation step, this grows further in length and forms PTh [32] (Scheme 2).

The porous nature of PTh provides high surface area for Pt deposition on PTh/SS electrode. Using cyclic voltammetry, Pt nanoparticles were deposited on PTh/SS electrode at a scan rate of 0.05 Vs^{-1} between − 0.7 V and 1.7 V vs SCE for 15 cycles (Fig. 2). In the case of Pt deposition, two redox couples were observed at 0.30 V and 0.49 V; 1.01 V and 1.36 V in the voltammograms. This suggests the presence of Pt in two oxidation states (Pt^{2+}/Pt^{4+}). Pt-deposited electrodes were cleaned with double-distilled water, dried, and further used for anodic oxidation of benzyl alcohol.

3.2 Voltammetric behavior of potassium ferrocyanide/ferricyanide at Pt–PTh/SS and PTh/SS electrodes

The cyclic voltammograms of $[Fe(CN)_6)]^{4-}/[Fe(CN)_6]^{3-}$ at Pt–PTh/SS, PTh/SS, and bare SS electrodes were studied at a scan rate of 0.05 Vs^{-1} (Fig. 3). The obtained CV data was used to find the surface area of the electrodes. Graphs were drawn by plotting anodic peak currents against square root of scan rate, and their respective slopes were determined. Randles–Sevcik equation (Eq. 1) was used to calculate the electrochemically active surface areas of the electrodes using

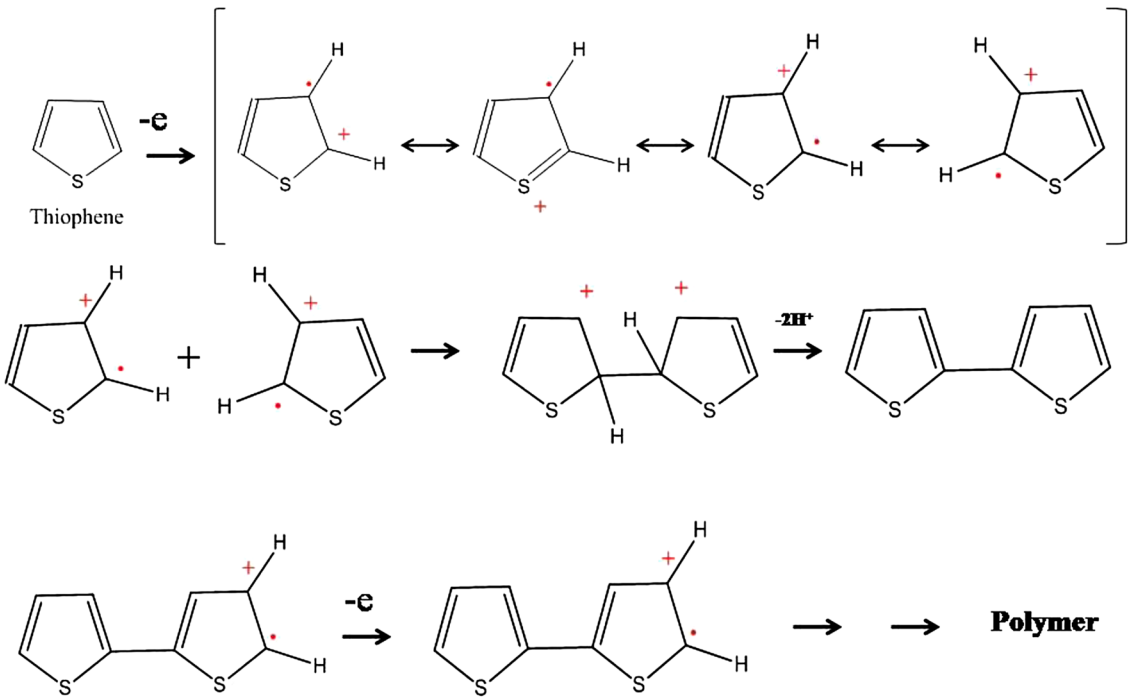

Scheme 2 Mechanism of electropolymerization of Thiophene [32]

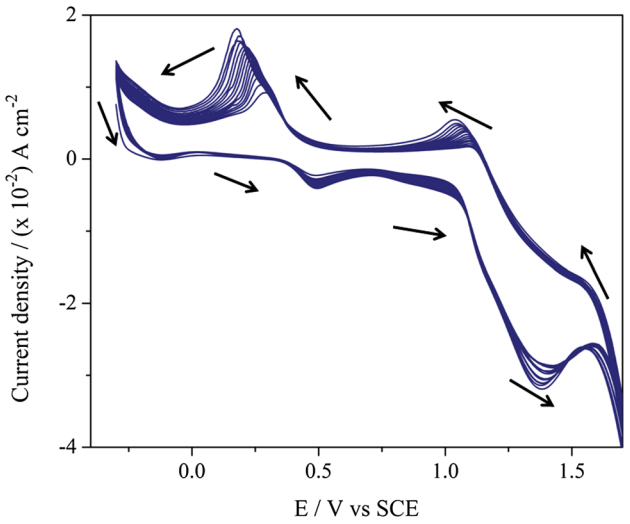

Fig. 2 Electrodeposition of Pt on PTh/SS electrode by 15 scanning potential cycles at a scan rate of 0.05 Vs^{-1}: (0.005 M) H_2PtCl_6; (0.1 M) H_2SO_4

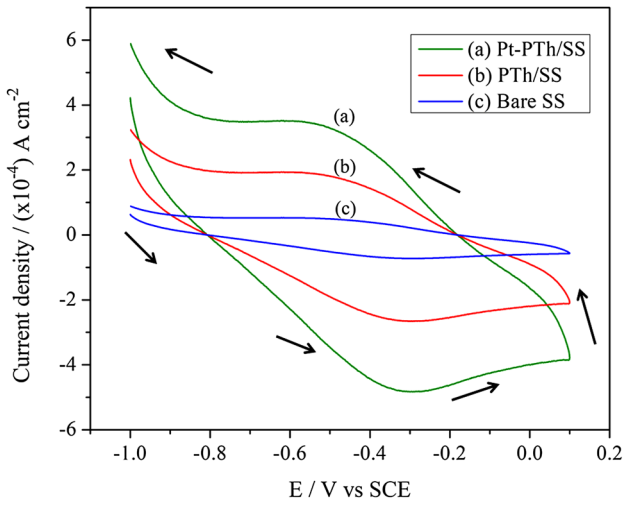

Fig. 3 Cyclic voltammograms of 1 mM potassium ferrocyanide/ferricyanide at Pt–PTh/SS (curve **a**), PTh/SS (curve **b**), and bare SS (curve **c**) electrodes in 1 M KCl

respective slopes, concentrations, and diffusion coefficient (0.76×10^{-5} cm^2/s).

$$i_p = 2.69 \times 10^5 A D_0^{1/2} n^{3/2} \nu^{1/2} C, \quad (1)$$

where A represents electroactive surface area in cm^2, D_0 is the diffusion coefficient in cm^2/s, n is the number of electrons participating in the redox reaction, ν is the scan rate in Vs^{-1} and C is the concentration of $K_4[Fe(CN)_6]/K_3[Fe(CN)_6]$ in the bulk solution in mol/cm^3. The value of electroactive surface area calculated for bare SS, PTh/SS, and Pt–PTh/SS electrodes are 0.42, 1.51, and 3.64 cm^2, respectively. Based on the results, it is understood that the surface area is very low for bare SS electrode, and the surface areas are high for PTh/SS and Pt–PTh/SS electrodes which can be attributed to the highly porous morphology of PTh, which also helps in the uniform dispersion of Pt nanoparticles.

3.3 EIS behavior of Pt–PTh/SS, PTh/SS, and bare SS electrodes

EIS is an effective technique to characterize the interfacial properties of the electrodes. The Nyquist plots of Pt–PTh/SS (curve a), PTh/SS (curve b), and bare SS (curve c) in 1 mM $K_4[Fe(CN)_6]/K_3[Fe(CN)_6]$ using 1 M KCl as electrolyte are shown in Fig. 4. The charge-transfer resistance (R_{CT}) is the semicircular diameter of the Nyquist plot. R_{CT} value of bare SS was about 630.0 Ω, whereas the R_{CT} value of PTh/SS was 150.0 Ω. This value greatly reduced to 112.6 Ω in case of Pt–PTh/SS. Therefore, it is evident that as R_{CT} value decreases, conducting nature increases. On modification with PTh, the conducting property is enhanced to a large extent. The electrodeposition of Pt on PTh/SS further decreased the R_{CT} value and increased its conductivity. Therefore, it can be concluded that the modification of bare SS with PTh and Pt–PTh/SS enhances the conductivity toward the redox process of $K_4[Fe(CN)_6]/K_3[Fe(CN)_6]$. Hence, it may possibly facilitate a good platform for electrocatalytic oxidation of benzyl alcohol. The equivalent-circuit parameters and errors of fitting of EIS data are given in Table 1.

3.4 Physicochemical characterization of modified electrodes

3.4.1 SEM and TEM analyses

SEM analyses of PTh/SS and Pt–PTh/SS electrodes are shown in Fig. 5a, b, respectively. The SS surface was uniformly covered with PTh and displayed flake-like morphology. PTh flakes on SS act as nucleation centers for the formation of Pt nanoclusters. The nanoclusters of Pt act as high-energy surface sites in attracting the molecules of benzyl alcohol toward the surface of the electrode. These metal nanoclusters provide channels for benzyl alcohol molecules to diffuse into the polymer matrix.

TEM image of Pt nanoclusters on PTh/SS is presented in Fig. 5c. It shows uniformly active surface growth of Pt nanoparticles on PTh modified SS electrode. Pt deposition further increased the surface area of electrode and facilitated diffusion of benzyl alcohol toward PTh/SS leading to an effective electrocatalytic oxidation process.

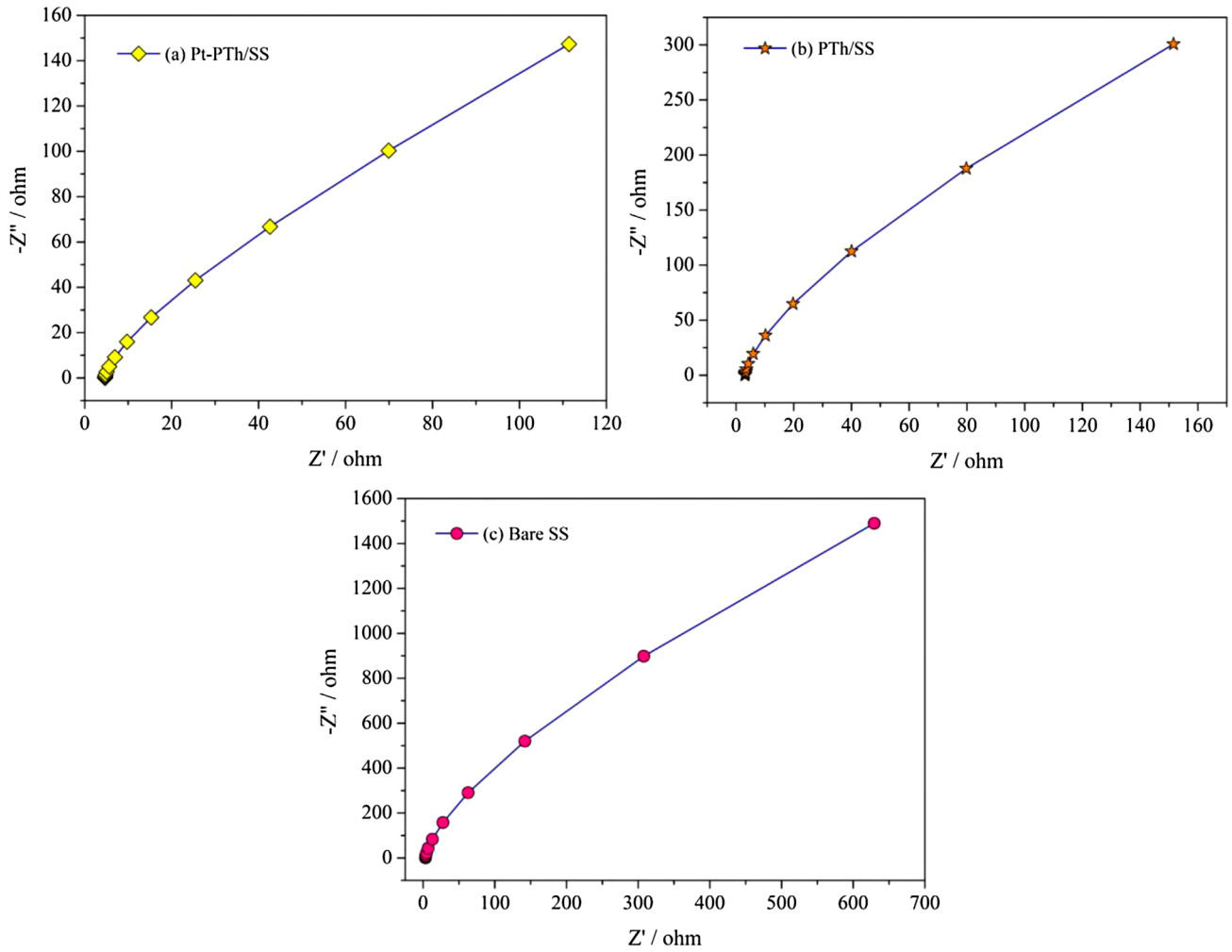

Fig. 4 Nyquist plots of **a** Pt–PTh/SS, **b** PTh/SS, and **c** bare SS electrodes in 1 mM $K_4[Fe(CN)_6]/K_3[Fe(CN)_6]$ using 1 M KCl as electrolyte

Table 1 The list of equivalent-circuit parameters with errors of fitting for the EIS data

Electrodes	Equivalent-circuit parameter	Values obtained	Fitted values	± Error
Bare SS	R_s (Ω)	33.460	33.438	0.0216
	R_{CT} (Ω)	630	629.8	0.1392
	C_{dl} (Ω^{-1} s)	0.001	0.007	0.003
	W	5.265×10^{-3}	0.0051	0.0001
PTh/SS	R_s (Ω)	0.3143	0.3121	0.0022
	R_{CT} (Ω)	150	149.8	0.1728
	C_{dl} (Ω^{-1} s)	0.0459	0.0457	0.0002
	W	7.4×10^{-2}	0.0739	0.0001
Pt–PTh/SS	R_s (Ω)	0.4818	0.4688	0.0130
	R_{CT} (Ω)	112.6	112.4	0.1562
	C_{dl} (Ω^{-1} s)	0.0791	0.0788	0.0003
	W	1.82×10^{-2}	0.0017	0.0001

3.4.2 XRD studies

The XRD pattern for Pt-PTh/SS electrode is given in Fig. 6. Peaks observed at 2θ values of 11.6° (222), 12.2° (100), 20.7° (111) and 34.1° (222) confirms the deposition of PTh on SS. The electrodeposited Pt peaks at 2θ values of 39.6°, 46.3° and 67.8° can be assigned to (111), (200) and (220) planes, respectively. The JCPDS number of Pt is 04-08-02 and it has fcc lattice. The sharp nature of peaks reveals that the depositions are crystalline in nature. The average crystallite size of Pt-Pth particles on SS electrode was found using the largest diffraction peak (11.6°) by Scherrer equation (Eq. 2).

$$L = K\lambda/\beta\cos\theta, \tag{2}$$

where L is the average crystallite size, K is the constant related crystallite shape, which is usually 0.9, λ represents the X-ray wavelength (0.1540 nm), β is the peak width at half maximum intensity in radiance, and θ is the angle of

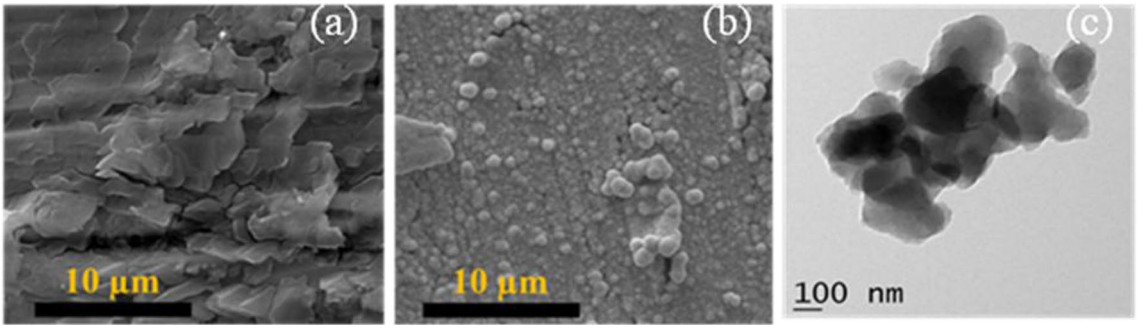

Fig. 5 SEM images of **a** PTh/SS **b** Pt–PTh/SS electrodes, and **c** TEM image of Pt–PTh/SS electrode

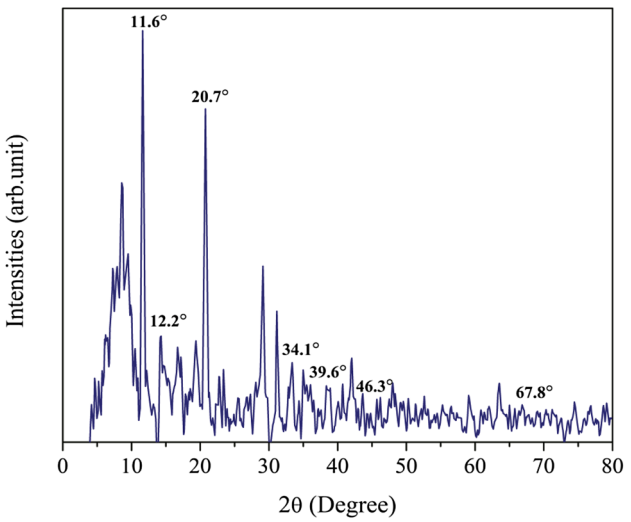

Fig. 6 XRD pattern of Pt–PTh/SS electrode

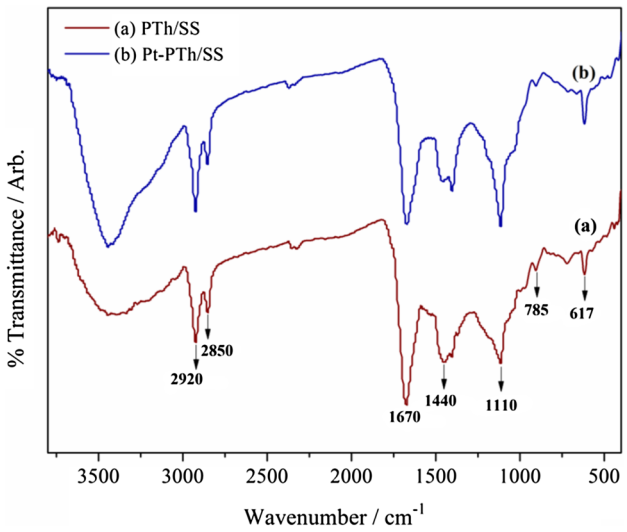

Fig. 7 FTIR spectra of PTh/SS (**a**) and Pt–PTh/SS (**b**)

incidence of the incoming X-ray. The average crystallite size determined using Scherrer equation was found to be 0.2397 nm.

3.4.3 IR and Raman spectroscopic studies

The IR spectra of PTh/SS and Pt–PTh/SS are depicted in Fig. 7. C–S stretching is observed at 785 and 617 cm^{-1}. C=C characteristic peak is seen at 1670 cm^{-1} and C–H plane deformation is observed at 1110 cm^{-1}. The peak at 1440 cm^{-1} is characteristic of thiophene ring stretching. Peaks at 2850 and 2920 cm^{-1} can be attributed to C–H stretching. The IR spectrum of Pt-PTh/SS also shows similar peaks with lower intensity when compared to PTh/SS. This indicates the absence of a chemical interaction between PTh and Pt nanoparticles at the electrode surface. The Raman spectrum of Pt–PTh/SS is shown in Fig. 8. The peaks at 1500 cm^{-1} and 700 cm^{-1} indicate C–H stretching and C–C stretching of thiophene ring, respectively. The sharp peak at 1458 cm^{-1} is typical of C=C symmetric stretching. The

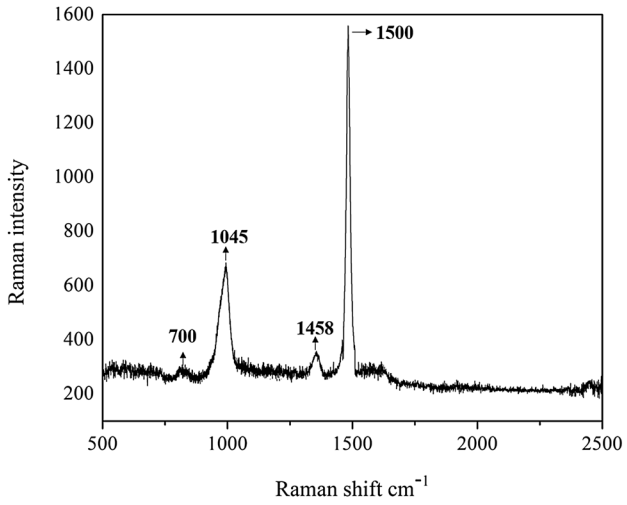

Fig. 8 Raman spectrum of Pt–PTh/SS

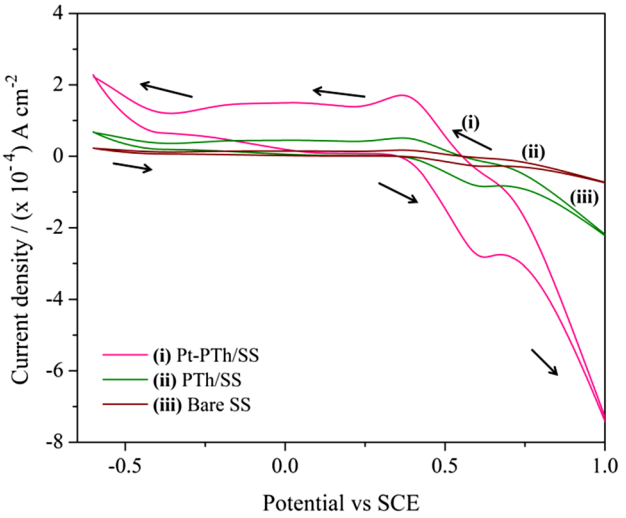

Fig. 9 Cyclic voltammograms of 0.01 M TEMPO at (i) Pt–PTh/SS (ii) PTh/SS, and (iii) bare SS in the absence of 10 mM benzyl alcohol with (0.1 M) $LiClO_4$ in acetonitrile medium

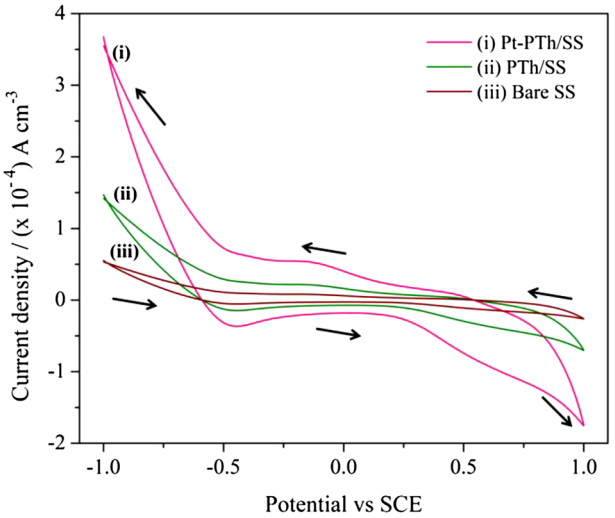

Fig. 10 Cyclic voltammograms of 0.01 M TEMPO at (i) Pt–PTh/SS (ii) PTh/SS, and (iii) bare SS in the presence of 10 mM benzyl alcohol with (0.1 M) $LiClO_4$ in acetonitrile medium

aromatic C–S stretching peak is observed at 1045 cm^{-1}. Similarly, IR spectrum of Pt deposition on PTh/SS does not show any prominent shift in peaks, which indicates that Pt is adsorbed onto PTh/SS electrode surface. This confirms that there is no chemical interaction between Pt and PTh.

3.5 Electrocatalytic oxidation of benzyl alcohol at Pt–PTh/SS electrode

Cyclic voltammetric experiments were performed to investigate the electrocatalytic oxidation of benzyl alcohol at Pt–PTh/SS, PTh/SS, and bare SS electrodes. The experiment was performed at a scan rate of 0.05 Vs^{-1} in 0.01 M TEMPO with $LiClO_4$ in acetonitrile medium. Cyclic voltammograms for 0.01 M TEMPO with 0.1 M $LiClO_4$ supporting electrolyte in acetonitrile at Pt–PTh/SS, PTh/SS, and bare SS in the absence of benzyl alcohol is depicted in Fig. 9. It can be observed from the cyclic voltammograms that TEMPO displays small current flow through bare SS and PTh/SS electrodes, whereas a broad voltammogram was obtained for Pt–PTh/SS. In the presence of benzyl alcohol, the oxidation of TEMPO becomes irreversible, and oxidation peak appears to be wavelike. Benzyl alcohol gives a weak current response for bare SS electrode and PTh/SS electrode in comparison to Pt–PTh/SS electrode (Fig. 10). Molecules of benzyl alcohol were greatly attracted toward the electrode surface due to high-energy active sites produced by Pt nanoparticles. Benzaldehyde obtained from the oxidation of benzyl alcohol at Pt–PTh/SS electrode was analyzed. This was done by analyzing the solution containing products of oxidation obtained on

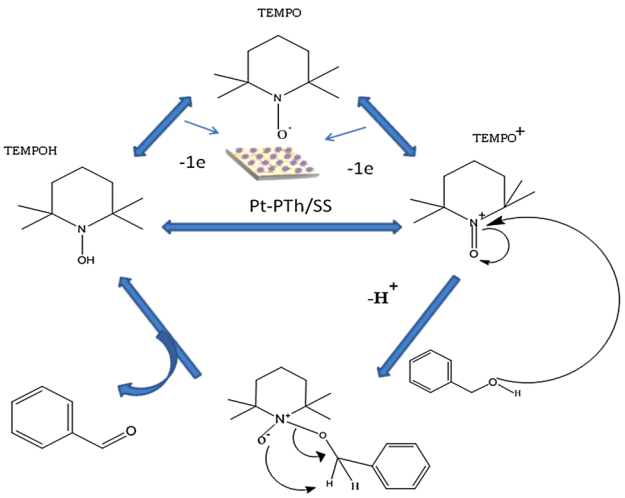

Scheme 3 Mechanism of benzyl alcohol oxidation at Pt–PTh/SS electrode using TEMPO

prolonged electrolysis (48 h) of 10 mM benzyl alcohol in the presence of TEMPO by HPLC using a Shimadzu LC-SA column (250 mm × 4.6 mm) as the stationary phase. The product purity was determined to be 85%. TEMPO gets oxidized to $TEMPO^+$ cation, and it acts as an initiator for the benzyl alcohol oxidation [33]. It selectively oxidizes benzyl alcohol to benzaldehyde and prevents further oxidation to benzoic acid. $TEMPO^+$ is reduced to TEMPOH, a hydroxyl amine obtained by $2e^-$ transfer at the electrode surface, and it directly gets converted to TEMPO. The mechanism of benzyl alcohol oxidation at Pt–PTh/SS electrode using TEMPO is given in Scheme 3.

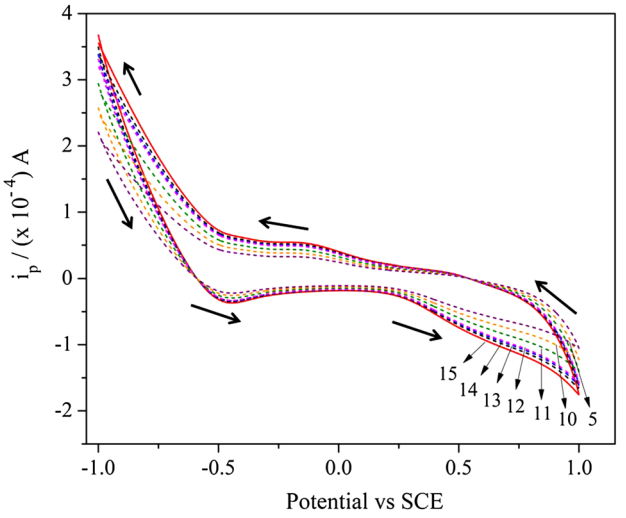

Fig. 11 Cyclic voltammograms of 0.01 M TEMPO in the presence of benzyl alcohol at different number of voltammetric cycles of Pt deposition on PTh/SS electrode

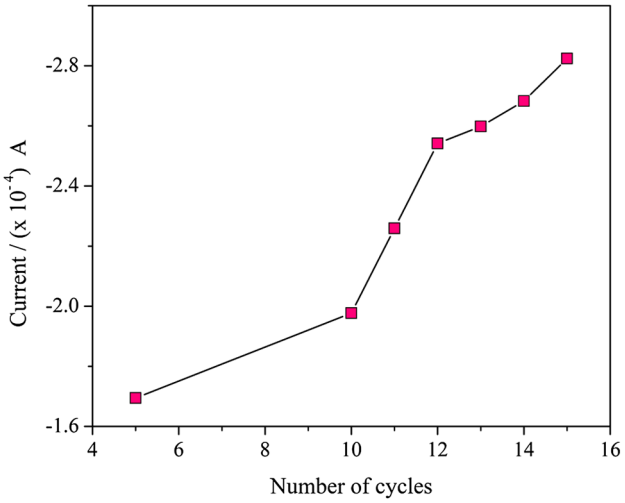

Fig. 12 Effect of the number of voltammetric cycles on the anodic peak current of 0.01 M TEMPO in the presence of benzyl alcohol at Pt–PTh/SS

3.6 Effect of number of cycles

The oxidation of 10 mM benzyl alcohol in the presence of TEMPO using Pt–PTh/SS electrode was studied for different number of cycles such as 5, 10, 11, 12, 13, 14, and 15 required for the deposition of Pt on PTh/SS electrode. With the increasing number of cycles for depositing Pt on PTh/SS electrode, the increased oxidation peak currents of TEMPO in the presence of benzyl alcohol were also observed. The potential was found to shift toward negative values up to 15 cycles after which the current remained constant. Therefore, 15 cycles were taken as optimal number of cycles for Pt deposition on PTh/SS for benzyl alcohol oxidation (Figs. 11, 12).

3.7 Effect of scan rate

The effect of scan rate on the oxidation of benzyl alcohol in the presence of TEMPO was studied at Pt–PTh/SS electrode using $LiClO_4$ supporting electrolyte in acetonitrile medium. Cyclic voltammograms of 0.01 M TEMPO in the presence of 10 mM benzyl alcohol at 0.02 Vs^{-1}, 0.04 Vs^{-1}, 0.05 Vs^{-1}, 0.06 Vs^{-1}, 0.08 Vs^{-1}, 0.1 Vs^{-1} and 0.12 Vs^{-1} are shown in Fig. 13. A linear graph was obtained for logarithm of peak currents plotted against logarithm of scan rates (Fig. 14). The results indicated that the electrochemical process was adsorption controlled and not diffusion controlled.

3.8 Reproducibility and stability

The reproducibility of electrode response was studied. Six electrodes were modified, and their electrochemical

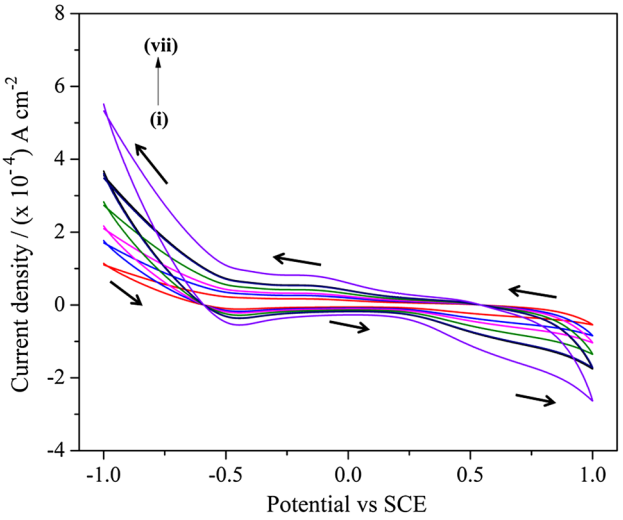

Fig. 13 Cyclic voltammograms of 0.01 M TEMPO in the presence of benzyl alcohol at Pt–PTh/SS electrode at scan rates (i) 0.02 Vs^{-1}, (ii) 0.04 Vs^{-1}, (iii) 0.05 Vs^{-1}, (iv) 0.06 Vs^{-1}, (v) 0.08 Vs^{-1}, (vi) 0.1 Vs^{-1}, (vii) 0.12 Vs^{-1}

responses toward benzyl alcohol oxidation in the presence of TEMPO were evaluated for 1 month at the interval of 5 days. The results revealed that the electrodes were stable for a longer period and were found to be effective in the electrooxidation of benzyl alcohol. A decrease of about 3% in the CV response of the electrode revealed its good stability. 50 continuous cycles were performed using cyclic voltammetry for Pt–PTh/SS electrode in the absence of benzyl alcohol, which has been depicted in Fig. 15.

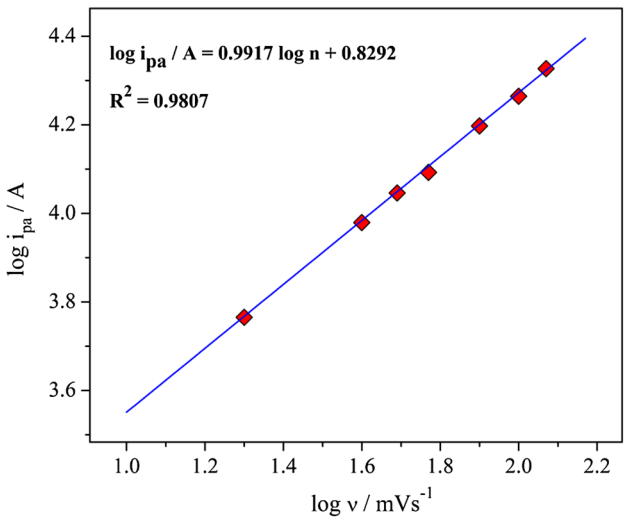

Fig. 14 Plot of logarithm of the anodic peak currents against logarithm of scan rates

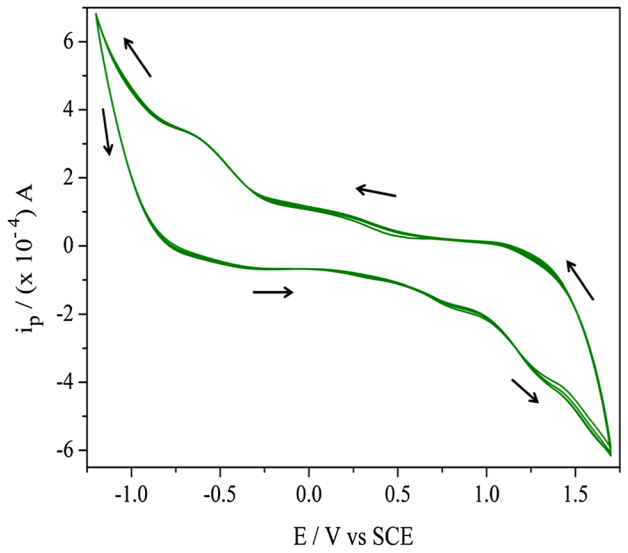

Fig. 15 CV response of 50 continuous cycles of Pt–PTh/SS electrode without TEMPO and benzyl alcohol in (0.1 M) $LiClO_4$ in acetonitrile

4 Conclusions

Electrocatalytic activity of Pt–PTh/SS electrode toward benzyl alcohol oxidation in the presence of TEMPO was studied using cyclic voltammetry. Pt electrodeposited on PTh-coated SS was present as nanoclusters uniformly dispersed on the electrode surface. The Pt nanoparticles act as high-energy surface sites in attracting the benzyl alcohol molecules toward the electrode surface. The cyclic voltammetric studies indicated that Pt–PTh/SS electrode is several times more efficient than bare SS electrode toward oxidation of benzyl alcohol mediated by TEMPO. Direct oxidation of benzyl alcohol to benzaldehyde could be achieved by a single step at Pt–PTh/SS electrode using TEMPO as a mediator in the proposed method.

Acknowledgements The authors are grateful to AFMM, IISc and MNCF, CeNSe, and IISc, Bengaluru for providing facilities for SEM, XRD, Raman spectroscopic and FT-IR analyses, respectively. The authors would like to thank STIC-SAIF, Cochin University, Kochi for TEM analysis.

References

1. Selvaraj V, Alagar M, Hamerton I (2007) Nanocatalysts impregnated polythiophene electrodes for the electrooxidation of formic acid. Appl Catal B 73:172–179. https://doi.org/10.1016/j.apcatb.2006.07.020
2. Kelaidopoulu A, Papoutsis A, Kokindas G, Napporn WT, Leger J-M, Lamy C (1999) Electrooxidation of β-D (+) glucose on bare and upd modified platinum particles dispersed in polyaniline. J Appl Electrochem 29:101–107. https://doi.org/10.1023/A:1003433206439
3. Tsakova V, Milchev A (1991) Electrochemical formation and stability of polyaniline films. Electrochim Acta 36:1579–1583. https://doi.org/10.1016/0013-4686(91)85009-V
4. Bose CSC, Rajeshwar K (1992) Efficient electrocatalyst assemblies for proton and oxygen reduction: the electrosynthesis and characterization of polypyrrole films containing nanodispersed platinum particles. J Electroanal Chem 333:235–256. https://doi.org/10.1016/0022-0728(92)80394-J
5. Tourillion G, Garnier F (1984) Inclusion of metallic aggregates in organic conducting polymers. A new catalytic system, [poly (3-methylthiophene)-Ag-Pt], for proton electrochemical reduction. J Phys Chem 88:5281–5285. https://doi.org/10.1021/j150666a034
6. Laborde H, Leger J-M, Lamy C (1994) Electrocatalytic oxidation of methanol and C1 molecules on highly dispersed electrodes Part 1: platinum in polyaniline. J Appl Electrochem 24:219–226. https://doi.org/10.1007/BF00242887
7. Oyama N, Anson FC (1979) Polymeric ligands as anchoring groups for the attachment of metal complexes to graphite electrode surfaces. J Am Chem Soc 101:3450–3456. https://doi.org/10.1021/ja00507a005
8. Abruna HD, Denisevich P, Umana M, Meyer JJ, Murray RW (1981) Rectifying interfaces using two-layer films of electrochemically polymerized vinylpyridine and vinylbipyridine complexes of ruthenium and iron on electrodes. J Am Chem Soc 103:1–5. https://doi.org/10.1021/ja00391a001
9. Zhu ZZ, Wang Z, Li HL (2008) Functional multi walled carbon nanotube/polyaniline composite films as supports of platinum for formic acid electrooxidation. Appl Surf Sci 54:2934–2940. https://doi.org/10.1016/j.apsusc.2007.10.033
10. Harish S, Mathiyarasu J, Phani KLN, Yeganaraman V (2009) Synthesis of conducting polymer supported Pd nanoparticles in aqueous medium and catalytic activity towards 4-nitrophenol reduction. Catal Lett 128:197–202. https://doi.org/10.1007/s10562-008-9732-x
11. Li C, Bai H, Shi G (2009) Conducting polymer nanomaterials: electrosynthesis and applications. Chem Soc Rev 38:2397–2409. https://doi.org/10.1039/B816681C
12. Reddy KR, Byung S, Kwang R, Jin-Chun K, Chung H, Lee Y (2009) Conducting polymer functionalized multi-walled carbon

nanotubes with noble metal nanoparticles: synthesis, morphological characteristics and electrical properties. Synth Met 159:595–603. https://doi.org/10.1016/j.synthmet.2008.11.030
13. Joice EK, Anitha V, Sudhakar YN, Bala G, Joseph S (2018) Poly (aniline) decorated with nanocactus platinum on carbon fiber paper and its electrocatalytic behavior toward toluene oxidation. J Electrochem Soc 165:H399–H406. https://doi.org/10.1149/2.1121807jes
14. Lemos HG, Santos SF, Venancio EC (2015) Polyaniline-Pt and polypyrrole-Pt nanocomposites: effect of supporting type and morphology on the nanoparticles size and distribution. Synth Met 203:22–30. https://doi.org/10.1016/j.synthmet.2015.02.006
15. Cao Y, Qiu J, Smith P (1995) Effect of solvents and co-solvents on the processibility of polyaniline: I. Solubility and conductivity studies. Synth Met 69:187–190. https://doi.org/10.1016/0379-6779(94)02412-R
16. Kausar A (2016) Electromagnetic interference shielding of polyaniline/Poloxalene/carbon black composite. Int J Mater Chem 6:6–11
17. Rahman MA, Kumar P, Park DS, Shim YB (2008) Electrochemical sensors based on organic conjugated polymers. Sensors 8:118–141. https://doi.org/10.3390/s8010118
18. Kazuyoshi T, Tokushige S, Shenglong W, Tokio Y (1988) A study of the electropolymerization of thiophene. Synth Met 24:203–215. https://doi.org/10.1016/0379-6779(88)90258-5
19. Ballav N, Biswas M (2003) Preparation and evaluation of a nanocomposite of polythiophene with Al_2O_3. Polym Int 52:179–184. https://doi.org/10.1002/pi.1001
20. Waltman RJ, Bargon J, Daiz AF (1983) Electrochemical studies of some conducting polythiophene films. J Phys Chem 87:1459–1463. https://doi.org/10.1021/j100231a035
21. Dai Y, Zhu F, Zhang H, Ma H, Wang W, Lei J (2016) Electrosynthesis and characterization of polythiophene and corrosion protection for stainless steel. Int J Electrochem Sci 11:4084–4091. https://doi.org/10.20964/110376
22. Kost KM, Bartak DE, Kazee B, Kuwana T (1988) Electrodeposition of platinum microparticles into polyaniline films with electrocatalytic applications. Anal Chem 60:2379–2384. https://doi.org/10.1021/ac00172a012
23. Dominguez SD, Pardilla JA, Murcia AB, Morallon E, Amoros DC (2008) Electrochemical deposition of platinum nanoparticles on different carbon supports and conducting polymers. J Appl Electrochem 38:259–268. https://doi.org/10.1007/s10800-007-9435-9
24. Schrebler R, Delvalle MA, Gomez H, Veas C, Cordova R (1995) Preparation of polythiophene-modified electrodes by electrodeposition of Pt and Pt + Pb. Application to formic acid electro-oxidation. J Electroanal Chem 380:219–227. https://doi.org/10.1016/0022-0728(94)03628-G
25. Swathirajan S, Mikhail YM (1992) Methanol oxidation on Platinum-Tin catalysts dispersed on poly(3-methyl)thiophene conducting polymer. J Electrochem Soc 139:2105–2110. https://doi.org/10.1149/1.2221186
26. Wang F, Xu J, Li X, Gao J, Zhuo L, Ohnishi R (2005) Liquid phase oxidation of toluene to benzaldehyde with molecular oxygen over copper-based heterogeneous catalysts. Adv Synth Catal 347:1987–1992. https://doi.org/10.1002/adsc.200505107
27. Nehamiah J, Sengupta S, Basu JK (2009) Selective production of benzaldehyde by permanganate oxidation of benzyl alcohol using 18-crown-6 as phase transfer catalyst. J Mol Catal A: Chem 309:153–158. https://doi.org/10.1016/j.molcata.2009.05.009
28. Zhou C, Chen Y, Guo Z, Wang X, Yang Y (2011) Promoted aerobic oxidation of benzyl alcohol on CNT supported platinum by iron oxide. Chem Commun 47:7473–7475. https://doi.org/10.1039/C1CC12264A
29. Herath AC, Becker JY (2008) 2,2,6,6-Tetramethylpiperidine-1-oxyl (TEMPO)-mediated catalytic oxidation of benzyl alcohol in acetonitrile and ionic liquid 1-buthyl-3-methyl-imidazolium hexafluorophosphate [BMIM][PF6]: kinetic analysis. Electrochem Acta 53:4324–4330. https://doi.org/10.1016/j.electacta.2007.12.082
30. Green WA, Hills Cousins JT, Richard CD, Brown Pletcher D, Leach SG (2013) A voltammetric study of the 2, 2, 6, 6-tetramethylpiperidin-1-oxyl (TEMPO) mediated oxidation of benzyl alcohol in tert-butanol/water. Electrochem Acta 113:550–556. https://doi.org/10.1016/j.electacta.2013.09.070
31. Dikalov SI, Dikalov AE, Manson RP (2002) Noninvasive diagnostic tool for inflammation-induced oxidative stress using electron spin resonance spectroscopy and an extracellular cyclic hydroxylamine. Arch Biochem Biophys 402:218–226. https://doi.org/10.1016/S0003-9861(02)00064-4
32. Wei Y, Chan CC, Tian J, Jang GW, Hsueh KF (1991) Electrochemical polymerization of thiophenes in the presence of bithiophene or terthiophene: kinetics and mechanism of the polymerization. Chem Mater 3:888–897. https://doi.org/10.1021/cm00017a026
33. Luca LD, Giacomelli G, Simonetta M, Andrea P (2003) Trichloroisocyanuric/TEMPO oxidation of alcohols under mild conditions: a close investigation. J Org Chem 68:4999–5001. https://doi.org/10.1021/jo034276b